

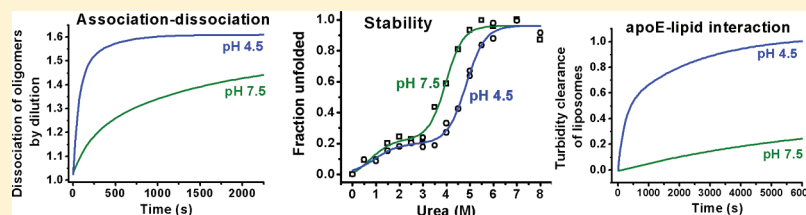
# Self-Association and Stability of the ApoE Isoforms at Low pH: Implications for ApoE–Lipid Interactions

Kanchan Garai, Berevan Baban, and Carl Frieden\*

Department of Biochemistry and Molecular Biophysics, Washington University School of Medicine, St. Louis, Missouri 63110, United States

**S** Supporting Information

## ABSTRACT:



Apolipoprotein E (apoE) isoforms are known to differentially accumulate in the lysosomes of neuronal cells, and the deleterious effects of the apoE4 isoform in Alzheimer's disease may relate to its properties at the low lysosomal pH. However, the effect of pH on the molecular properties of full-length apoE is unclear. Here we examine the pH dependence of the monomer–dimer–tetramer reaction, of lipid binding, and of the stability of the three major apoE isoforms. Using FRET measurements, we find that the association–dissociation behavior of apoE proteins changes dramatically with changes in pH. At pH 4.5, approximating the pH of the lysosome, rate constants for association and dissociation are 2–10 times faster than those at pH 7.4. Aggregation beyond the tetrameric form is also more evident at lower pH values. Stability, as measured by urea denaturation at pH 4.5, is found to be considerably greater than that at neutral pH and to be isoform dependent. Lipid binding, as measured by turbidity clearance of unilamellar vesicles of DMPC, is faster at acidic pH values and consistent with our previous hypothesis that it is only the monomeric form of apoE that binds lipid tightly. Since apoE is more stable at pH 4.5 than at neutral pH, the more rapid apoE–lipid interactions at low pH are not correlated with the stability of the apoE isoforms, but rather to the faster association–dissociation behavior. Our results indicate that pathological behavior of apoE4 may arise from altered molecular properties of this protein at the acidic pH of the lysosome.

Apolipoprotein E (apoE), a 299-residue protein, is a constituent of lipoproteins both in the periphery and in the central nervous system (CNS) playing key roles in lipids and cholesterol transport. In the CNS apoE is the major lipoprotein associated with high-density lipoprotein (HDL)-like particles. The apoE lipoprotein particles deliver cholesterol and lipids to neurons and play critical roles in the maintenance of neuronal health. There are three common isoforms apoE2, apoE3, and apoE4 which differ by cysteine to arginine changes at positions 112 and 158. ApoE2 has cysteines and apoE4 has arginines at both these positions while apoE3 has a cysteine at position 112 and an arginine at position 158. The apoE isoforms differ significantly in terms of their roles in Alzheimer's disease (AD) and cardiovascular diseases with apoE4 being the major risk factor for AD while apoE3 is considered normal and apoE2 appears to be protective.<sup>1–9</sup> How apoE4 influences the pathology of AD remains unclear, but several lines of evidence indicate a direct interaction of the apoE isoforms with the amyloid- $\beta$  (A $\beta$ ) peptide.<sup>10–15</sup> Biochemical analysis of the amyloid plaques in AD brains showed extensive association of apoE proteins with A $\beta$  peptides,<sup>11</sup> indicating a direct role of apoE in the aggregation of A $\beta$ . A recent study using apoE target

replacement mice showed AD-like pathology following inhibition of an A $\beta$  degrading enzyme, neprilysin, in apoE isoform specific manner.<sup>15</sup> Mice expressing apoE4 showed elevated levels of apoE4, A $\beta$ , and the lysosome specific enzyme cathepsin D in the hippocampal region of the mouse brain.<sup>15</sup> Lysosomal dysfunction and accumulation of acid hydrolases in the neocortical pyramidal neurons is an early marker of AD.<sup>16</sup> ApoE4 but not apoE3 is shown to potentiate lysosomal leakage by A $\beta$  in the cell culture studies.<sup>13</sup> Thus, interactions between apoE4 and A $\beta$  as a consequence of their accumulation in lysosomes may be important in the pathology of AD.

Structural and functional properties of the apoE proteins have been extensively studied at neutral pH over the last three decades. The stability and lipid-binding behavior of the truncated N-terminal domain of the apoE isoforms are significantly altered at acidic pH<sup>17,18</sup> but biophysical studies on the full-length apoE proteins at acidic pH values are lacking. This is an important issue

**Received:** May 2, 2011

**Revised:** June 23, 2011

**Published:** June 23, 2011

because changes in structural properties at acidic pH has been hypothesized to cause destabilization of lysosomal membranes particularly by apoE4.<sup>13</sup>

Although there is no published structure of the full-length protein, apoE molecules consist of an N- and a C-terminal domain linked by a protease sensitive hinge region. The N-terminal domain (residues 1–191) contains the polymorphism sites (residues 112 and 158) and contains the receptor binding site.<sup>19</sup> The C-terminal domain is believed to contain the lipid-binding, self-association, and A $\beta$ -binding sites.<sup>11,20–24</sup> Using five mutations in the C-terminal domain, Wang and co-workers have prepared a monomeric form of full-length apoE3<sup>25</sup> and have recently determined the structure of this isoform by solution NMR (Wang, J, personal communication). This structure shows extensive interactions between the N- and C-terminal domains.

Lipid-free apoE self-associates to form oligomers through its C-terminal domain.<sup>21,26</sup> We have previously shown that self-association of apoE can be described by a monomer–dimer–tetramer model. We have also determined the individual rate constants at neutral pH<sup>27</sup> and have shown that self-association of lipid-free apoE critically influences the kinetics of lipidation since dissociation of the apoE oligomers to monomer is prerequisite to lipidation of apoE.<sup>28</sup>

Here we investigate the effect of pH on self-association, lipidation, and stability of the apoE proteins. The rate constants of the self-association process, which can be described by a monomer–dimer–tetramer model, are found to be 2–10 times faster at pH 4.5 compared to those at neutral pH. Examination of pH-dependent lipidation kinetics and stability of the apoE isoforms reveals a strong correlation of lipidation kinetics with dissociation of oligomers to monomer and not with stability. Additionally, there is a slow aggregation of apoE observed at concentrations as low as 100 nM at pH 4.5 which appears to be nonspecific but which may be physiologically important.

## MATERIALS AND METHODS

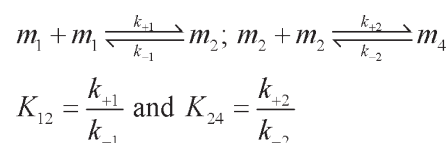
**Expression and Purification of Recombinant ApoE.** ApoE was prepared and purified as described previously.<sup>29</sup> Site-directed mutations were introduced by QuickChange site-directed mutagenesis kit (Stratagene). The sequences of mutant proteins were verified by DNA sequencing. All chemicals used were Ultrapure from Sigma-Aldrich (St. Louis, MO).

**Passivation of Cuvette Surface.** To avoid adsorption of apoE, the inner surface of the quartz cuvette used for fluorescence experiments was passivated according to Selvin and Ha.<sup>27,30</sup>

**Fluorescence Labeling of ApoE.** Alanine at position 102 in apoE4 was mutated to cysteine for fluorescent labeling. This single cysteine of apoE4 was labeled by either Alexa488 maleimide or Alexa546 maleimide (Invitrogen) as described previously.<sup>27</sup> For labeling apoE3 and apoE2, the cysteine residue(s) were mutated to serine and alanine at position 102 was mutated to cysteine. In this way, all apoE proteins were labeled at the same position. We have previously shown that the effects of these mutations and the fluorescence labeling on the association–dissociation behavior of the WT-apoE are minimal.<sup>27</sup> For all the samples the labeling efficiency was greater than 90%.

**Dissociation Kinetics of ApoE Using Intermolecular FRET.** Phosphate buffers at pH 6.0, 6.5, 7.0, and 7.5 were prepared using NaH<sub>2</sub>PO<sub>4</sub> and Na<sub>2</sub>HPO<sub>4</sub> in appropriate amounts. For experiments at pH 4.0, 4.5, 5.0, and 5.5, buffers were prepared using sodium acetate and acetic acid in appropriate amounts. The apoE

## Scheme 1. Self-Association Model of ApoE Consisting of Monomer–Dimer–Tetramer<sup>a</sup>



<sup>a</sup>  $m_1$ ,  $m_2$ , and  $m_4$  represent monomer, dimer, and tetramer, respectively.  $K_{12}$  and  $K_{24}$  are equilibrium constants for the monomer to dimer and dimer to tetramer association processes.

dissociation kinetic experiments were performed using intermolecular FRET as described previously.<sup>27</sup> Briefly, apoE (A102C)-labeled proteins with either Alexa488 or Alexa546 were mixed at a ratio of 1:1 in HEPES buffer at pH 7.4. For pH-dependent kinetic experiments 10  $\mu$ M fluorescently labeled apoE stock solution was diluted to 20 nM in 20 mM phosphate (pH 6.0, 6.5, 7.0, or 7.5) or acetate (pH 4.0, 4.5, 5.0, and 5.5) buffer containing 150 mM NaCl and 0.1%  $\beta$ -mercaptoethanol ( $\beta$ Me). Time-dependent changes in FRET were monitored using excitation and emission monochromators set to 490 and 520 nm, respectively. For determination of rate constants at pH 4.5 varying amounts of labeled apoE4 stock solution (from 1.2 to 80  $\mu$ L of 10  $\mu$ M apoE) were added into 2.4 mL of 20 mM acetate buffer containing 150 mM NaCl and 0.1%  $\beta$ -mercaptoethanol ( $\beta$ Me). All experiments were performed at 25  $^{\circ}$ C.

**Analysis of the Kinetic Data.** The kinetics data were fit with Kintek Explorer (KinTek Corp.) using the model in Scheme 1.<sup>31</sup> The errors in the parameter values were calculated from the covariance matrix values obtained from data fitting.<sup>32</sup>

**Preparation of Unilamellar Liposomes.** Small unilamellar vesicles (SUV) of dimyristoyl-*sn*-glycero-3-phosphocholine (DMPC) were prepared by extrusion through 50 nm polycarbonate membranes (Avanti Polar Lipids Inc.) followed by centrifugation at 14 kg. These liposomes, when tested by light scattering, are stable for several days at room temperature.

**Turbidity Measurements.** WT-apoE4 was diluted from a 10  $\mu$ M stock solution to 100 nM in phosphate or acetate buffers (20 mM phosphate or acetate, 150 mM NaCl, 0.1%  $\beta$ Me, and pH 7.5 to 4.5) containing 0.12 mg/mL small unilamellar vesicles of DMPC at 25  $^{\circ}$ C. The turbidity clearance of the DMPC liposomes was performed by monitoring scattering from the sample as has been described previously.<sup>28</sup>

**Denaturation Experiments Using Tryptophan Fluorescence.** For urea denaturation studies using the fluorescence of the native tryptophans a 10  $\mu$ M apoE stock solution in 6 M urea, 20 mM Hepes, 0.1%  $\beta$ Me, and pH 7.5 buffer was diluted to 50 nM final concentration into 20 mM phosphate, pH 7.5, or 20 mM acetate, pH 4.5, buffer containing varying concentrations of urea. Fluorescence data were recorded at 335 nm with excitation at 290 nm. The fraction ( $f$ ) of unfolded population was calculated from

$$f = \frac{I - I_U}{I_N - I_U} \quad (1)$$

where  $I$  is the fluorescence intensity at 335 nm and “U” and “N” indicating unfolded and native state, respectively. Nonlinear least-squares fit was performed using Origin 7.0 (Origin Laboratories) with a three-state model and the equation adapted from Morjana

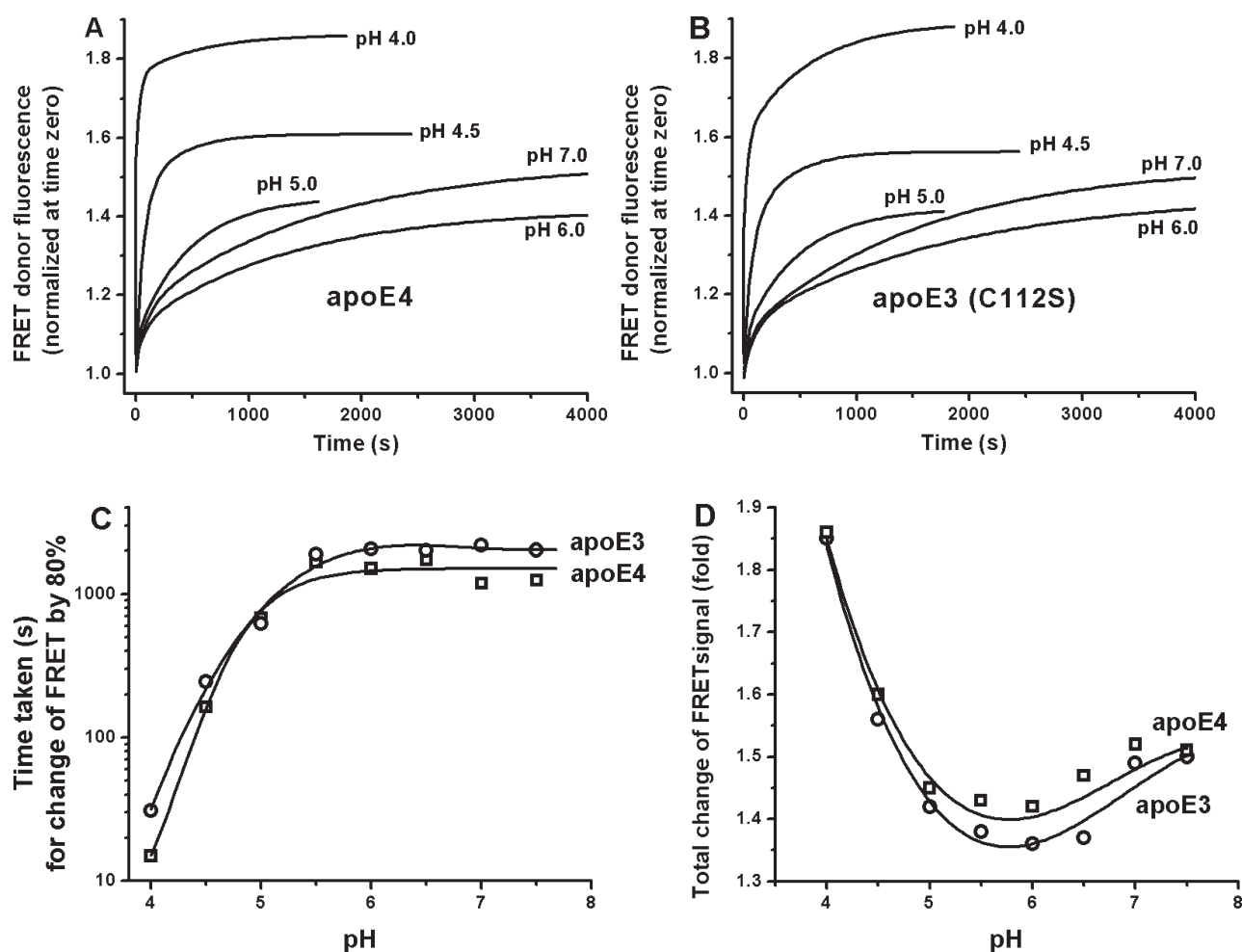


**Figure 1.** Kinetics of dissociation of apoE oligomers as a function of pH. A 10  $\mu$ M stock solution of apoE4(A102C) or apoE3(C112S/A102C) labeled with Alexa488 or Alexa546 and mixed in a 1:1 ratio in 20 mM Hepes, pH 7.4 buffer was diluted to 20 nM final concentration into 20 mM acetate (pH 4.0, 4.5, 5.0, and 5.5) or 20 mM phosphate (pH 7.5, 7.0, 6.5, and 6.0) buffer containing 150 mM NaCl and 0.1%  $\beta$ Me. Fluorescence of FRET donor was monitored as a function of time. (A, B) Fits of the dissociation data with two exponentials. For clarity, raw data are not shown. (C) Time required for a change of FRET signal by 80% of total and (D) fold increase of the FRET signal measured by ratio of final to initial donor fluorescence for apoE4 ( $\square$ ) and apoE3(C112S) ( $\circ$ ). The solid lines in (C) and (D) are polynomial fits to data and do not carry any meaning. Alexa488 fluorescence was monitored at 520 nm with excitation at 490 nm.

et al.<sup>33</sup> The errors in the parameter values are calculated from the covariance matrix values obtained from data fitting.<sup>32</sup>

## RESULTS

**Effect of pH on Self-Association.** We have previously described the self-association of apoE molecules at neutral pH using a monomer–dimer–tetramer model.<sup>27</sup> The rate constants of the monomer–dimer–tetramer model were determined from kinetic experiments using intermolecular FRET between apoE molecules fluorescently labeled with either a donor or an acceptor dye. The results obtained from the FRET experiments at neutral pH were found to be consistent with sedimentation equilibrium, sedimentation velocity, and fluorescence correlation spectroscopy measurements.<sup>27</sup> We now examine the self-association behavior of the apoE isoforms as a function of pH using FRET. ApoE proteins labeled with Alexa488 or Alexa546 were mixed at pH 7.4 in a 1:1 ratio and then diluted from 10  $\mu$ M to a final concentration of 20 nM in buffers ranging from pH 4.0 to 7.5. Figure 1A,B presents data showing that at all pH values

FRET donor fluorescence increases in a time-dependent manner, consistent with dissociation of oligomeric apoE to lower molecular weight forms. At every pH, there are two distinct phases. As discussed previously, we interpret the faster phase as due to dissociation of tetramers to dimers and the slower phase due to dissociation of dimers to monomers.<sup>27</sup> As shown in Figure 1A,B both the kinetic behavior and the total extent of change of the FRET signal are pH-dependent. Plots of the time required for a 80% change in FRET signal as a function of pH show that the dissociation becomes faster below pH 5.5 (Figure 1C). Figure 1D shows that the extent of dissociation of the apoE oligomers as measured by the total change of the FRET signal (i.e.,  $F_{t=\infty}/F_{t=0}$ ) is also pH-dependent with the minima around pH 6.0. The larger extent in FRET signal change at pH 4 suggests that apoE oligomers do not dissociate completely to monomer even at concentrations as low as 20 nM at pH values above pH 4. Taken together, Figures 1A–D show that association–dissociation behavior of apoE is dramatically influenced by changes in pH.

**Effect of Salt on Self-Association.** Figure 2A shows a small effect of salt on the rate of dissociation at pH 7.4 but little or no

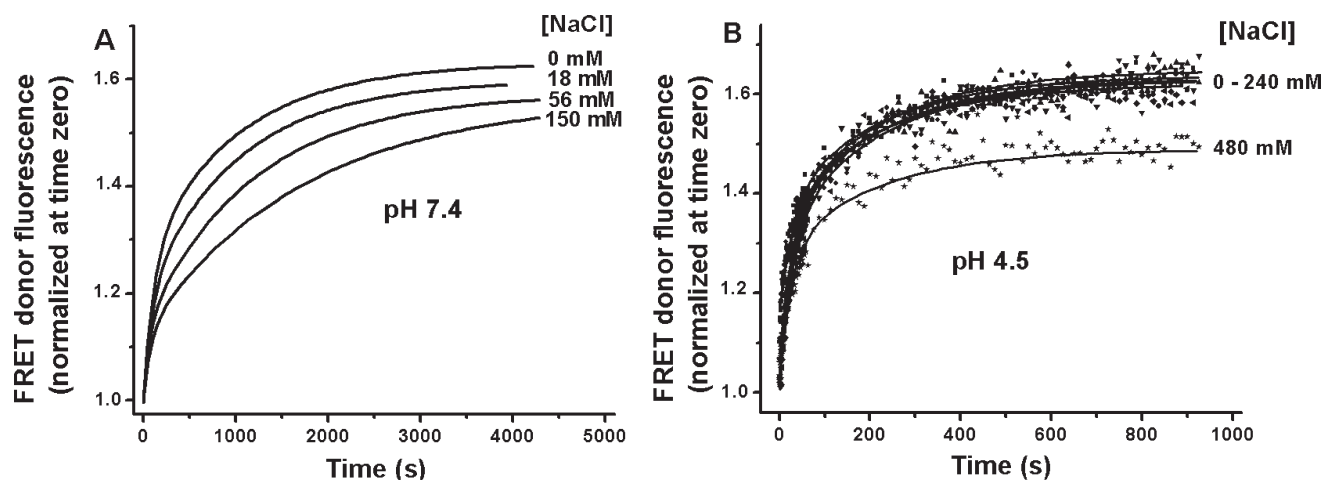


**Figure 2.** Kinetics of dissociation of apoE4 as a function of NaCl concentration. A 5  $\mu$ M stock solution of fluorescently labeled apoE4 prepared in Hepes, pH 7.4, buffer was diluted to 20 nM final concentration into (A) 20 mM phosphate, pH 7.4, or (B) 20 mM acetate, pH 4.5, buffer containing varying amounts of NaCl as shown in the figures. The symbols represent data, and the solid lines are two exponential fits of the data. Only fits are shown in (A) for clarity. Experiments performed in the same way as described in the legend of Figure 1.

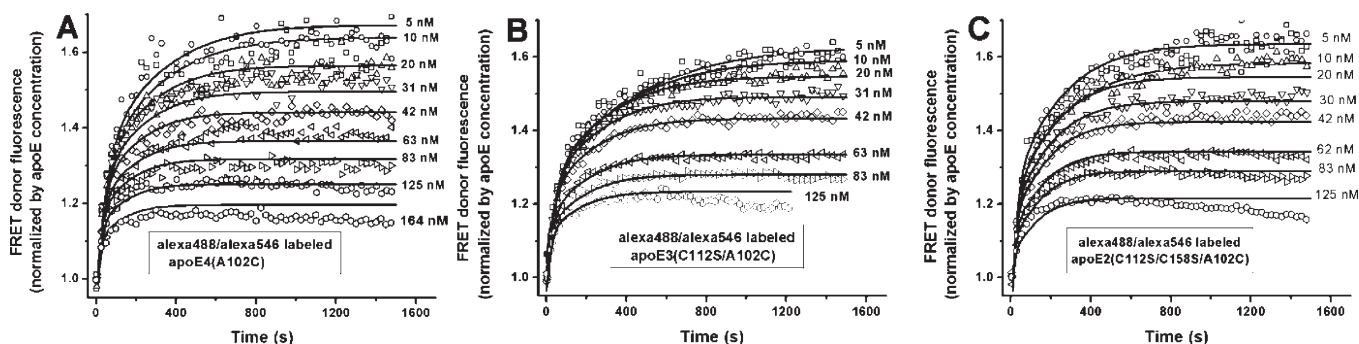


**Figure 3.** Kinetics of dissociation apoE isoforms at pH 4.5. A 10  $\mu$ M fluorescently labeled apoE stock solution prepared in Hepes, pH 7.4, buffer was diluted into 20 mM acetate buffer, pH 4.5, 150 mM NaCl, and 0.1%  $\beta$ Me to varying final concentrations as indicated in the figures. The symbols represent data for (A) apoE4, (B) the serine mutant of apoE3 (C112S), and (C) the serine mutant of apoE2 (C112S/C158S). The solid lines are fit to a monomer–dimer–tetramer model shown in Scheme 1 using Kintek Explorer<sup>53</sup> and the rate constants listed in Table 1. Experiments performed in the same way as described in the legend of Figure 1.

effect at pH 4.5, suggesting that electrostatic interactions are not the primary determinant of monomer–monomer interactions in this pH range. Although a high salt concentration (480 mM) at pH 4.5 is shown to decrease the total extent of dissociation, the apparent rate of dissociation does not appear to be affected.

**Determination of Individual Rate Constants at pH 4.5.** In order to determine the individual rate constants at pH 4.5, the dissociation experiments were performed at various concentrations of apoE as described previously.<sup>27</sup> The data for apoE4 (A102C), apoE3(C112S/A102C), and apoE2(C112S/C158S/A102C) are shown in parts A, B, and C of Figure 3, respectively. These data were obtained by diluting a 10  $\mu$ M fluorescently labeled apoE solution to various final concentrations as shown in the figure. The stock solution is prepared in HEPES buffer at pH 7.4 to avoid aggregation which, at pH 4.5, occurs above  $\approx$ 100 nM for all the isoforms of apoE (see below). As discussed earlier, the kinetic data show two phases corresponding to dissociation of tetramers to dimers and dimers to monomers. The data at all concentrations ( $\approx$ 5–100 nM) are fit globally to the monomer–dimer–tetramer model as shown in Scheme 1. The values of the individual rate constants obtained from the analysis, as

summarized in Table 1, indicate that both association and dissociation rate constants are faster than those previously determined at pH 7.4 at similar apoE concentrations.<sup>27</sup> In addition, the rate constants differ between the apoE isoforms, indicating isoform specificity. Although the differences between the individual rate constants between isoforms appear to be small compared to the errors, differences are clear in some of the rate constants such as in the monomer to dimer association rate constant ( $k_{+1}$ ) and in the tetramer to dimer dissociation rate constant ( $k_{-2}$ ) (see Table 1). In addition, the monomer–dimer dissociation constant  $K_{12}^{-1}$ , the reciprocal of the equilibrium constant, is significantly different between the apoE isoforms being smallest ( $74 \pm 26$  nM) for apoE4 and largest ( $236 \pm 45$  nM) for apoE2. Altogether, differences between apoE2 with the other two isoforms are more pronounced than between apoE3 and apoE4.

**Aggregation of ApoE at pH 4.5.** The data in Figure 3A–C show that at the higher concentrations of apoE there is gradual decrease of the donor fluorescence starting at  $\sim$ 800 s. Figure 4 shows data over longer times (10 000 s) for apoE4. Here, 10  $\mu$ M fluorescently labeled protein was diluted to 164 nM into pH 4.5



**Table 1. Rate and Equilibrium Constants of Self-Association of ApoE Isoforms at pH 4.5**

sample	$k_{+1}$ ( $\times 10^4$ M $^{-1}$ s $^{-1}$ )	$k_{-1}$ ( $\times 10^{-3}$ s $^{-1}$ )	$k_{+2}$ ( $\times 10^5$ M $^{-1}$ s $^{-1}$ )	$k_{-2}$ ( $\times 10^{-2}$ s $^{-1}$ )	$K_{12}^{-1}$ ( $\times 10^{-9}$ M)	$K_{24}^{-1}$ ( $\times 10^{-9}$ M)
apoE4 <sup>a</sup>	1.9 $\pm$ 0.01	1.4 $\pm$ 0.5	4.2 $\pm$ 0.5	1.3 $\pm$ 0.1	74 $\pm$ 26	31 $\pm$ 4
apoE3 <sup>a,b</sup>	1.4 $\pm$ 0.01	1.9 $\pm$ 0.5	5.0 $\pm$ 0.5	1.5 $\pm$ 0.1	135 $\pm$ 35	30 $\pm$ 3
apoE2 <sup>a,c</sup>	1.1 $\pm$ 0.01	2.6 $\pm$ 0.5	7.6 $\pm$ 0.5	2.6 $\pm$ 0.1	236 $\pm$ 45	29 $\pm$ 3

<sup>a</sup> Alexa488- or Alexa546-labeled apoE(A102C) and mixed with 1:1 ratio. <sup>b</sup> Serine mutant of apoE3, i.e., apoE3(C112S). <sup>c</sup> Serine mutant of apoE2, i.e., apoE2(C112S/C158S).

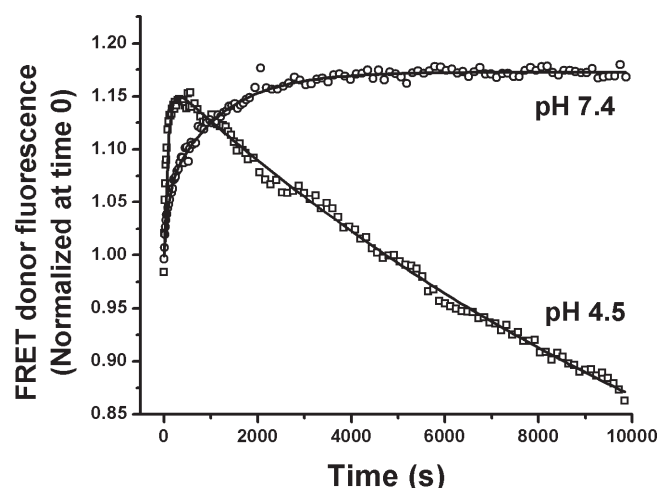


**Figure 4.** Kinetics of dissociation and aggregation of apoE4 at pH 4.5 and 7.4. A 10  $\mu$ M fluorescently labeled apoE stock solution prepared in 20 mM Hepes, pH 7.4, buffer was diluted to 164 nM into 20 mM acetate, pH 4.5, or 20 mM phosphate, pH 7.4, buffer in the presence of 150 mM NaCl, 0.1%  $\beta$ Me. The symbols represent data and the solid lines fits of the data by two exponentials. Experiments performed in the same way as described in the legend of Figure 1. The time course is 10-fold longer than that shown in Figure 3.

buffer. After the initial increase, consistent with dissociation of the tetramers to dimers and monomers, the fluorescence then slowly decreases, taking more than 3 h to go to completion. Superimposed is the plot obtained from a similar experiment performed at pH 7.4, showing initial increase of fluorescence without loss of fluorescence signal at longer times (Figure 4). Thus, the observed loss of fluorescence at pH 4.5 cannot be due to bleaching of the fluorescent probe. Atomic force microscopy (AFM) images of the material observed at these long time at pH 4.5 appear as amorphous aggregates showing no particular morphology, rather than as defined species such as tetramers (Supporting Information Figure S1). Such aggregation at these apoE levels does not occur at pH 7.4<sup>29</sup> and may be an important component in the toxic function of the protein at low pH values.

**Stability of ApoE Isoforms as a Function of pH.** Figure 5 shows urea denaturation plots of 50 nM WT-apoE isoforms as measured by changes in tryptophan fluorescence. The denaturation plots for all three isoforms of apoE show two-step (three-state) unfolding which has been interpreted to be the unfolding of the C-terminal domain, followed by the unfolding of the N-terminal domain.<sup>34</sup> The data were fit with a three-state model, referred to as native (N), intermediate (I), and unfolded (U), according to Morjana et al.<sup>33</sup> Free energies,  $m$  values, and the denaturation midpoints ( $DM_{N-I}$  and  $DM_{I-U}$ ) are summarized in Table 2. It is clear from  $DM_{I-U}$  values in Table 2 (and also from the stability curves in Figure 5) that the stability of all the

apoE isoforms is greater at pH 4.5 than at pH 7.5. In addition, the stability between the apoE isoforms is different at both pH values with apoE2 being the most stable and apoE4 being the least. The  $DM_{N-I}$  values, which are considered to denote the stability of the C-terminal domain,<sup>34</sup> do not appear to differ significantly between the isoforms or between the neutral and acidic pH. The differences in the  $m$  values, which is a parameter of cooperativity of unfolding, between the isoforms do not appear to be significant although differences in the  $m$  values have been reported recently when using guanidinium hydrochloride denaturation at neutral pH.<sup>35</sup> The denaturation midpoint values at pH 7.5 are consistent with published results.<sup>28,34,36</sup> Previously reported data at low pH, however, used only the N-terminal domain,<sup>18</sup> and the nature of the denaturation curve appears different when using the complete protein.

**Effect of pH and Salt on ApoE Lipidation.** We have previously shown that dissociation of the apoE oligomers to monomer is a necessary and rate-limiting step for lipidation of apoE.<sup>28</sup> Alternatively, it has been suggested that stability of the apolipoproteins is correlated with the lipidation process.<sup>37–39</sup> To test which view is more appropriate at lower pH, we performed lipidation experiments as a function of pH. The kinetics of lipidation of apoE was monitored by changes in turbidity of small unilamellar vesicles of DMPC after addition of 100 nM (final concentration) WT-apoE4 from a 10  $\mu$ M stock solution. This procedure can be used because lipid-free apoE solubilizes liposomes as a consequence of forming small disc-like lipoprotein particles (radius  $\sim$ 6 nm) that are no longer turbid.<sup>40–42</sup> Figure 6A shows that the rate of turbidity clearance changes dramatically with the changes in solution pH. It can be seen from Figure 1, which shows the kinetics of dissociation of the apoE oligomers, and Figure 6A, which shows the kinetics of lipidation of apoE, that faster rates of dissociation of oligomers lead to faster lipidation of apoE. Fast lipidation at pH 4.5 is also observed for apoE3 and apoE2 (Supporting Information Figure S2). However, comparison of the apoE isoforms is not possible due to the presence of nonspecific aggregation even at low concentrations ( $>100$  nM) of the apoE proteins at this pH. A small change in the lipidation kinetics is observed at pH 7.4 with change in salt concentration (Figure 6B), in agreement with the small change observed in the self-association kinetics under similar conditions (Figure 2A). Thus, the changes in kinetics of dissociation of apoE oligomers and the changes in the rates of lipidation of apoE occur concurrently.

## DISCUSSION

While apoE isoforms differ only by single amino acid changes only apoE4 is considered a risk factor for late onset Alzheimer's disease. A large body of data suggests that apoE modulates the A $\beta$  plaque pathology in AD brain by affecting A $\beta$  aggregation and/or by affecting the clearance of A $\beta$  aggregates from brain (reviewed

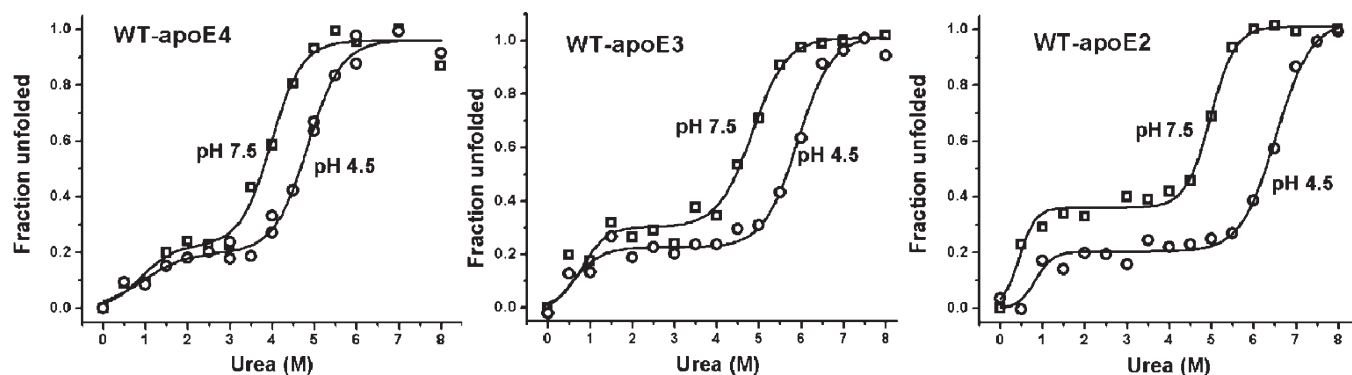


**Figure 5.** pH dependence of stability of the apoE isoforms by urea denaturation. Tryptophan fluorescence of 50 nM wild-type apoE4 or apoE3 or apoE2 was monitored as a function of urea concentration in 20 mM phosphate pH 7.5 or 20 mM acetate pH 4.5 buffer containing 150 mM NaCl and 0.1%  $\beta$ Me. The unfolded fractions were calculated using eq 1. The solid lines are fits to the data using a three-state denaturation model according to Morjana et al.<sup>33</sup> The results from the analysis are summarized in Table 2. Tryptophan fluorescence was monitored at 335 nm with excitation at 290 nm.

**Table 2.** Summary of the Stability Parameters Obtained from the Urea Denaturation Data

apoE isoform	pH	$\Delta G_{N \rightarrow I}^a$ (kcal/mol)	$\Delta G_{I \rightarrow U}^a$ (kcal/mol)	$m_{N \rightarrow I}^a$ (kcal/L)	$m_{I \rightarrow U}^a$ (kcal/L)	$DM_{N \rightarrow I}^b$ (mol/L of urea)	$DM_{I \rightarrow U}^b$ (mol/L of urea)
apoE4	7.5	$1.4 \pm 0.7$	$6.5 \pm 1.2$	$1.6 \pm 0.7$	$1.6 \pm 0.3$	$0.9 \pm 0.2$	$4.0 \pm 0.1$
apoE4	4.5	$1.1 \pm 0.5$	$7.2 \pm 0.9$	$1.2 \pm 0.4$	$1.5 \pm 0.2$	$0.9 \pm 0.2$	$4.8 \pm 0.1$
apoE3	7.5	$1.7 \pm 1.0$	$7.2 \pm 1.0$	$2.1 \pm 1.0$	$1.5 \pm 0.2$	$0.8 \pm 0.2$	$4.8 \pm 0.1$
apoE3	4.5	$1.0 \pm 0.4$	$8.8 \pm 1.5$	$1.8 \pm 0.6$	$1.5 \pm 0.2$	$0.6 \pm 0.1$	$5.9 \pm 0.2$
apoE2	7.5	$1.4 \pm 0.5$	$10.1 \pm 2.8$	$3.0 \pm 1.0$	$2.0 \pm 0.5$	$0.5 \pm 0.1$	$5.0 \pm 0.2$
apoE2	4.5	$2.5 \pm 0.3$	$9.4 \pm 1.5$	$3.0 \pm 1.0$	$1.4 \pm 0.2$	$0.8 \pm 0.2$	$6.5 \pm 0.2$

<sup>a</sup> N, I, and U refers to native, intermediate, and unfolded states of the protein, respectively.  $\Delta G$  and  $m$  values are calculated from analysis of the data presented in Figure 5 using a three-state model according to Morjana et al.<sup>33</sup> Errors are calculated using the covariance matrix obtained from data fitting.<sup>32</sup> <sup>b</sup> DM refers to denaturation midpoint, calculated as  $DM = \Delta G/m$ .<sup>52</sup> Errors are calculated using the covariance matrix obtained from data fitting.<sup>32</sup>

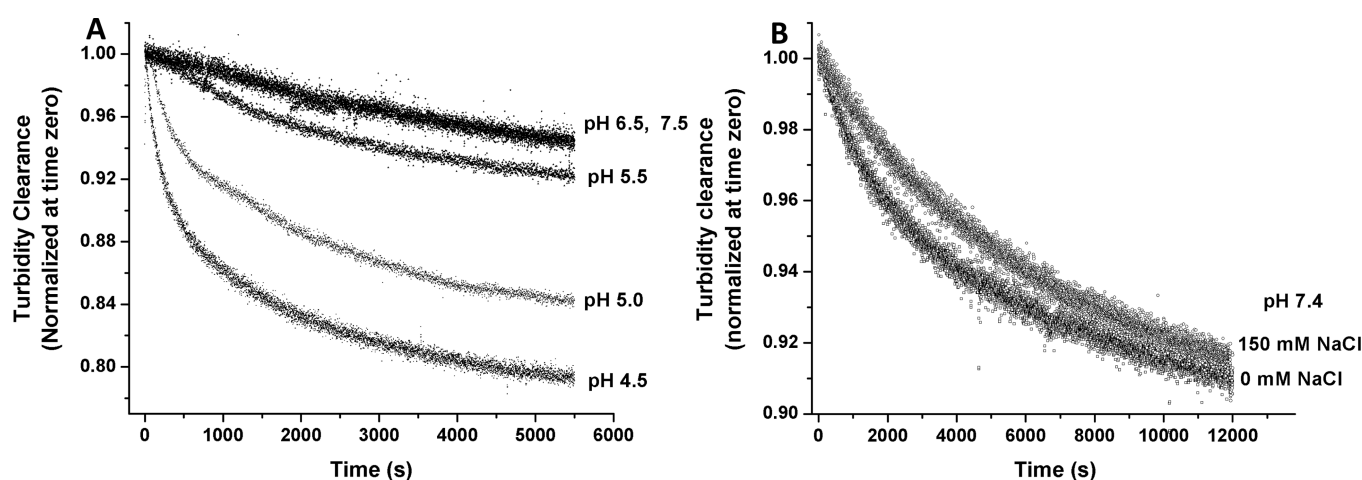


**Figure 6.** Effect of pH and salt on the kinetics of apoE lipidation.

(A) Turbidity measured by scattering from DMPC liposomes followed by addition of 100 nM WT-apoE4 diluted from a 10  $\mu$ M stock solution into a 0.12 mg/mL DMPC liposome solution into 20 mM phosphate (pH 7.5 and 6.5) or acetate (pH 5.5, 5.0, and 4.5) buffer containing 150 mM NaCl, 0.1%  $\beta$ Me. (B) Turbidity clearance by WT-apoE4 of liposomes in 20 mM phosphate pH 7.5 buffer in presence of 0 or 150 mM NaCl.

in ref 43). While the mechanism of the  $A\beta$ –apoE interaction is still unclear, it is generally believed that C-terminal domain of apoE interacts with  $A\beta$  and  $A\beta$  is shown to be colocalized with apoE in the lysosomes of neuronal cells in apoE target replacement mouse brain with AD pathology.<sup>15</sup> The acidic pH of

the lysosome and the presence of the apoE4 isoform were found to be crucial to  $A\beta$  induced disruption of the lysosomal membranes and release of toxic materials inside the cells.<sup>13</sup> In addition, lysosomal dysfunction and elevated amounts of lysosomes and late endosomes in the neurons is an early indicator of

AD brain.<sup>16</sup> However, the mechanism of the altered apoE- $A\beta$ -lysosome interactions has remained unexplored. In fact, the molecular properties of apoE isoforms have not been well studied under acidic pH conditions.

**Self-Association Behavior of ApoE at Low pH.** Studies at pH values closer to that of lysosomes and below the isoelectric point have not been reported. At pH 7.4, we have shown that a monomer-dimer-tetramer model can describe the self-association of apoE.<sup>27</sup> At this pH, the dissociation rate constants were found to be slow with dissociation of the dimer to monomer typically taking more than 1 h. The rate constants for monomer-monomer and dimer-dimer association were found to be  $\sim 10^4$  and  $10^5 \text{ M}^{-1} \text{ s}^{-1}$ , respectively, 1–2 orders of magnitude less than that expected from diffusion-limited self-association. Comparison of the rate constants at pH 4.5 with those at neutral pH shows that the rate constants are in general 2–10 times larger at pH 4.5. Presumably, the rate constants are further increased at pH 4.0 (see Figure 1A,B). Protonation of glutamate and aspartate residues (there are only two histidine residues, one of which is at the C-terminus) followed by disruption of intermolecular salt bridges is likely the primary cause behind the altered association-dissociation behavior of the apoE molecules at low pH, but it is not yet possible to determine which residues are responsible. Partial disruption of these salt bridges at low pH can account for faster dissociation of the apoE tetramers and dimers. Formation of intermolecular salt bridges may be a slow process leading to the observed slow association rate constants at neutral pH than that is expected from diffusion-limited process.<sup>27</sup>

**pH-Dependent Stability.** The stability of the apoE isoforms has been studied extensively at neutral pH, but similar data are lacking at low pH. Morrow et al. investigated the urea stability of the isolated N-terminal domain of apoE2, apoE3, and apoE4 at pH 4<sup>18</sup> and found the data for apoE4 and apoE3 to be fit only by a three-state model. They concluded that an intermediate present at urea concentrations near 4 M was a molten globule. Consequently, apoE has been considered to be a molten globule at low pH values, but in the absence of urea, there is no evidence for that conclusion. Indeed, our data show that the full-length apoE is more stable at acidic pH than at neutral pH and that the enhanced stability is observed for all the isoforms. The reason behind the enhanced stability is not clear but protonation of glutamate or aspartate residues which are buried in the four-helix bundle structure of the N-terminal domain<sup>44</sup> may account for this enhanced stability at low pH.

**Relationship between Self-Association, Stability, and Lipid Binding.** In spite of extensive studies with apolipoprotein and phospholipid interactions, the molecular mechanism of the apoE-lipid interaction process is still not clear. ApoE proteins undergo a large conformational opening upon binding to lipid.<sup>41</sup> On the basis of the data at neutral pH for several lipoproteins such as apolipoprotein III, apoA-I, and the three isoforms of apoE, it has been proposed that the stability of the apolipoproteins determines the kinetics of lipidation of these proteins.<sup>37–39,45</sup> Since opening of the helix-bundle motif of the lipid-free apoE is necessary for lipidation, it is believed that higher stability of the protein corresponds to a slower kinetics of lipid binding. We have previously shown that apoE-lipid interaction mechanism must include the self-association behavior and that dissociation of apoE oligomers to monomers is the rate-determining step in lipidation of apoE.<sup>28</sup> Our data as a function of pH and ionic strength reinforce this idea by showing that changes in the rate constants of self-association and in the rate of lipidation vary in

the same way (Figure 6 and Figures 1 and 2). Thus, the data are consistent with the view that dissociation of oligomers to monomers controls the lipidation process of apoE molecules. Our data show that faster lipid binding kinetics of apoE at acidic pH cannot be correlated with changes in stability of the protein at that pH. It is likely, however, that conformational changes of the N- and the C-terminal domains and in the domain-domain interaction occur at low pH (Frieden, C., and Garai, K., unpublished data). However, understanding those processes has been hindered due to lack of a published high resolution structure of full-length apoE.

**Oligomerization versus Aggregation.** We have shown that dilution of apoE from low  $\mu\text{M}$  concentrations to nM concentrations can be described as a monomer-dimer-tetramer process.<sup>27</sup> Yet it is known that higher molecular weight forms are present at higher protein concentrations. Hatters et al. have presented evidence that at 37 °C and concentrations above 6  $\mu\text{M}$  native tetramers form soluble aggregates at pH 7.4.<sup>46</sup> While these aggregates appear to have a different morphology than expected for amyloid fibrils, the rate of aggregate formation is isoform dependent with apoE4 aggregating more rapidly than apoE3. These aggregates appear to be toxic to neuronal cells. The authors suggest that the differences in rate of aggregate formation may relate to their physiological function. In addition, it is generally accepted that proteins tend to aggregate under conditions close to their isoelectric point. That appears to be the case for the apoE proteins. The isoelectric points of apoE isoforms, as measured by 2-D gel electrophoresis, ranges between 6.2 and 6.6, and Figures 3 and 4 provide evidence for aggregation of apoE isoforms even at concentrations as low as 100 nM at pH 4.5.

It is clear from our data that all three isoforms of apoE show aggregation propensity, faster rate constants for the monomer-dimer-tetramer process, increased stability, and more rapid association with phospholipid at pH 4.5. Although there are isoform specific differences, these differences are not large (see Table 1). Hence, differences in the pathogenic effects of apoE isoforms most likely arise due to differences in their intracellular concentration and/or due to differences in their association to the lysosomes. In the apoE target replacement mouse model the apoE4 level was elevated more than apoE3 in the brain regions which showed higher levels of  $A\beta$  peptides following inhibition of a  $A\beta$  degrading enzyme neprilysin.<sup>15</sup> In a cell culture model using human brain tissue up to 87% of the intraneuronal apoE4 was found to be colocalized with the lysosomal marker cathepsin D whereas only 9% of the apoE3 was colocalized.<sup>47</sup> Why intracellular or lysosome associated apoE4 levels are different is not clear, but differences in the intracellular trafficking,<sup>47</sup> in the rate of degradation,<sup>48,49</sup> and interactions with other proteins including  $A\beta$  peptides<sup>22,50</sup> due to differences in the structural properties as evidenced from its low stability compared to the other isoforms may be a cause. However, apoE4 accumulation in the lysosome could be pathogenic due to formation of aggregates and high affinity of lipid binding in the acidic pH of the lysosomes.

Altered interactions of the apoE isoforms with lipids or lipoproteins and  $A\beta$  are believed to be important factors in Alzheimer's and cardiovascular diseases. Since lipid or lipoprotein binding of apoE and interaction with amyloid- $\beta$  peptides are thought to occur through the C-terminal domain which is also involved in the self-association,<sup>20–22</sup> these processes may be expected to compete with each other under physiological conditions. In fact, apoE- $A\beta$  interaction has been shown to affect



the apoE–lipid interactions.<sup>51</sup> Our results presented here and elsewhere<sup>28</sup> suggest that interactions between the apoE molecules themselves may also play important roles to alter their physiological functions.

In conclusion, we have shown that stability, self-association, and lipidation behavior of the apoE isoforms are strongly sensitive to the pH of the solution. The individual rate constants of the monomer–dimer–tetramer model of self-association of the apoE isoforms have been determined. The data of the lipidation of apoE are consistent with the notion that dissociation of the apoE oligomers to monomer is crucial to lipidation of apoE. Additionally, at pH 4.5 a high propensity for nonspecific aggregation, which may have a pathogenic function, was observed.

## ■ ASSOCIATED CONTENT

**S Supporting Information.** Atomic force microscopy (AFM) image of the aggregates of apoE4 at pH 4.5 (Figure S1); phospholipid liposome solubilization by WT-apoE isoforms at pH 4.5 (Figure S2). This material is available free of charge via the Internet at <http://pubs.acs.org>.

## ■ AUTHOR INFORMATION

### Corresponding Author

\*E-mail: [frieden@biochem.wustl.edu](mailto:frieden@biochem.wustl.edu). Phone: (314) 362-3344. Fax: (314) 362-7183.

## ■ ACKNOWLEDGMENT

We thank Scott Crick for recording the atomic force microscopy images of the aggregates of apoE.

## ■ ABBREVIATIONS

AD, Alzheimer's disease; apoE, apolipoprotein E; WT, wild type;  $\beta$ Me,  $\beta$ -mercaptoethanol; DMPC, dimyristoyl-*sn*-glycero-3-phosphocholine; FRET, fluorescence resonance energy transfer; A $\beta$ , amyloid beta.

## ■ REFERENCES

- (1) Corder, E. H., Saunders, A. M., Pericak-Vance, M. A., and Roses, A. D. (1995) There is a pathologic relationship between ApoE-epsilon 4 and Alzheimer's disease. *Arch. Neurol.* 52, 650–651.
- (2) Corder, E. H., Saunders, A. M., Risch, N. J., Strittmatter, W. J., Schmechel, D. E., Gaskell, P. C., Jr., Rimmler, J. B., Locke, P. A., Conneally, P. M., and Schmechel, K. E. et al. (1994) et al. Protective effect of apolipoprotein E type 2 allele for late onset Alzheimer disease. *Nature Genet.* 7, 180–184.
- (3) Alberts, M. J., Graffagnino, C., McClenny, C., DeLong, D., Strittmatter, W., Saunders, A. M., and Roses, A. D. (1995) ApoE genotype and survival from intracerebral haemorrhage. *Lancet* 346, 575.
- (4) Farrer, L. A., Cupples, L. A., Haines, J. L., Hyman, B., Kukull, W. A., Mayeux, R., Myers, R. H., Pericak-Vance, M. A., Risch, N., and van Duijn, C. M. (1997) Effects of age, sex, and ethnicity on the association between apolipoprotein E genotype and Alzheimer disease. A meta-analysis. APOE and Alzheimer Disease Meta Analysis Consortium. *JAMA, J. Am. Med. Assoc.* 278, 1349–1356.
- (5) Drzezga, A., Grimmer, T., Henriksen, G., Muhlau, M., Perneczky, R., Miederer, I., Praus, C., Sorg, C., Wohlschlaeger, A., Riemenschneider, M., Wester, H. J., Foerstl, H., Schwaiger, M., and Kurz, A. (2009) Effect of APOE genotype on amyloid plaque load and gray matter volume in Alzheimer disease. *Neurology* 72, 1487–1494.

- (6) Davignon, J., Gregg, R. E., and Sing, C. F. (1988) Apolipoprotein E polymorphism and atherosclerosis. *Arteriosclerosis* 8, 1–21.
- (7) Mahley, R. W., Huang, Y., and Rall, S. C., Jr. (1999) Pathogenesis of type III hyperlipoproteinemia (dysbetalipoproteinemia). Questions, quandaries, and paradoxes. *J. Lipid Res.* 40, 1933–1949.
- (8) Bennet, A. M., Di Angelantonio, E., Ye, Z., Wensley, F., Dahlin, A., Ahlbom, A., Keavney, B., Collins, R., Wiman, B., de Faire, U., and Danesh, J. (2007) Association of apolipoprotein E genotypes with lipid levels and coronary risk. *JAMA, J. Am. Med. Assoc.* 298, 1300–1311.
- (9) Wagle, J., Farner, L., Flekkoy, K., Wyller, T. B., Sandvik, L., Eiklid, K. L., Fure, B., Stensrod, B., and Engedal, K. (2009) Association between ApoE epsilon4 and cognitive impairment after stroke. *Dement. Geriatr. Cogn. Disord.* 27, 525–533.
- (10) Strittmatter, W. J., Saunders, A. M., Schmechel, D., Pericak-Vance, M., Enghild, J., Salvesen, G. S., and Roses, A. D. (1993) Apolipoprotein E: high-avidity binding to beta-amyloid and increased frequency of type 4 allele in late-onset familial Alzheimer disease. *Proc. Natl. Acad. Sci. U. S. A.* 90, 1977–1981.
- (11) Naslund, J., Thyberg, J., Tjernberg, L. O., Wernstedt, C., Karlstrom, A. R., Bogdanovic, N., Gandy, S. E., Lannfelt, L., Terenius, L., and Nordstedt, C. (1995) Characterization of stable complexes involving apolipoprotein E and the amyloid beta peptide in Alzheimer's disease brain. *Neuron* 15, 219–228.
- (12) Holtzman, D. M., Bales, K. R., Tenkova, T., Fagan, A. M., Parsadanian, M., Sartorius, L. J., Mackey, B., Olney, J., McKeel, D., Wozniak, D., and Paul, S. M. (2000) Apolipoprotein E isoform-dependent amyloid deposition and neuritic degeneration in a mouse model of Alzheimer's disease. *Proc. Natl. Acad. Sci. U. S. A.* 97, 2892–2897.
- (13) Ji, Z.-S., Mullendorff, K., Cheng, I. H., Miranda, R. D., Huang, Y., and Mahley, R. W. (2006) Reactivity of Apolipoprotein E4 and Amyloid b Peptide. *J. Biol. Chem.* 281, 2683–2692.
- (14) Manelli, A. M., Bulfinch, L. C., Sullivan, P. M., and LaDu, M. J. (2007) Abeta42 neurotoxicity in primary co-cultures: Effect of apoE isoform and Abeta conformation. *Neurobiol. Aging* 28, 1139–1147.
- (15) Belinson, H., Lev, D., Masliah, E., and Michaelson, D. M. (2008) Activation of the Amyloid Cascade in Apolipoprotein E4 Transgenic Mice Induces Lysosomal Activation and Neurodegeneration Resulting in Marked Cognitive Deficits. *J. Neurosci.* 28, 4690–4701.
- (16) Nixon, R. A., Cataldo, A. M., Paskevich, P. A., Hamilton, D. J., Wheelock, T. R., and Kanaley-Andrews, L. (1992) The Lysosomal System in Neurons. *Ann. N.Y. Acad. Sci.* 674, 65–88.
- (17) Weers, P. M., Narayanaswami, V., and Ryan, R. O. (2001) Modulation of the lipid binding properties of the N-terminal domain of human apolipoprotein E3. *Eur. J. Biochem.* 268, 3728–3735.
- (18) Morrow, J. A., Hatters, D. M., Lu, B., Hochtl, P., Oberg, K. A., Rupp, B., and Weisgraber, K. H. (2002) Apolipoprotein E4 forms a multimeric globule. A potential basis for its association with disease. *J. Biol. Chem.* 277, 50380–50385.
- (19) Wilson, C., Wardell, M. R., Weisgraber, K. H., Mahley, R. W., and Agard, D. A. (1991) Three-dimensional structure of the LDL receptor-binding domain of human apolipoprotein E. *Science* 252, 1817–1822.
- (20) Westerlund, J. A., and Weisgraber, K. H. (1993) Discrete carboxyl-terminal segments of apolipoprotein E mediate lipoprotein association and protein oligomerization. *J. Biol. Chem.* 268, 15745–15750.
- (21) Aggerbeck, L. P., Wetterau, J. R., Weisgraber, K. H., Wu, C. S., and Lindgren, F. T. (1988) Human apolipoprotein E3 in aqueous solution. II. Properties of the amino- and carboxyl-terminal domains. *J. Biol. Chem.* 263, 6249–6258.
- (22) Strittmatter, W. J., Weisgraber, K. H., Huang, D. Y., Dong, L. M., Salvesen, G. S., Pericak-Vance, M., Schmechel, D., Saunders, A. M., Goldgaber, D., and Roses, A. D. (1993) Binding of human apolipoprotein E to synthetic amyloid beta peptide: isoform-specific effects and implications for late-onset Alzheimer disease. *Proc. Natl. Acad. Sci. U. S. A.* 90, 8098–8102.
- (23) Pillot, T., Goethals, M., Najib, J., Labeur, C., Lins, L., Chambaz, J., Brasseur, R., Vandekerckhove, J., and Rosseneu, M. (1999)  $\beta$ -Amyloid Peptide Interacts Specifically with the Carboxyl-Terminal Domain of Human Apolipoprotein E. *J. Neurochem.* 72, 230–237.



- (24) Barbier, A., Clement-Collin, V., Dergunov, A. D., Visvikis, A., Siest, G., and Aggerbeck, L. P. (2006) The structure of human apolipoprotein E2, E3 and E4 in solution 1. Tertiary and quaternary structure. *Biophys. Chem.* 119, 158–169.
- (25) Zhang, Y., Vasudevan, S., Sojitrawala, R., Zhao, W., Cui, C., Xu, C., Fan, D., Newhouse, Y., Balestra, R., Jerome, W. G., Weisgraber, K., Li, Q., and Wang, J. (2007) A monomeric, biologically active, full-length human apolipoprotein E. *Biochemistry* 46, 10722–10732.
- (26) Perugini, M. A., Schuck, P., and Howlett, G. J. (2000) Self-association of human apolipoprotein E3 and E4 in the presence and absence of phospholipid. *J. Biol. Chem.* 275, 36758–36765.
- (27) Garai, K., and Frieden, C. (2010) The Association-Dissociation Behavior of the ApoE Proteins: Kinetic and Equilibrium Studies. *Biochemistry* 49, 9533–9541.
- (28) Garai, K., Baban, B., and Frieden, C. (2011) Dissociation of apoE oligomers to monomers is required for high affinity binding to phospholipid vesicles. *Biochemistry* 50, 2550–2558.
- (29) Garai, K., Mustafi, S. M., Baban, B., and Frieden, C. (2010) Structural differences between apolipoprotein E3 and E4 as measured by <sup>19</sup>F NMR. *Protein Sci.* 19, 66–74.
- (30) Selvin, P. R., and Ha, T. (2008) *Single-Molecule Techniques: A Laboratory Manual*; Cold Spring Harbor Laboratory Press, Cold Spring Harbor, NY.
- (31) Johnson, K. A., Simpson, Z. B., and Blom, T. (2009) Global kinetic explorer: a new computer program for dynamic simulation and fitting of kinetic data. *Anal. Biochem.* 387, 20–29.
- (32) Meyer, S. (1992) *Data Analysis for Scientists and Engineers*, John Wiley & Sons Inc., New York.
- (33) Morjana, N. A., McKeone, B. J., and Gilbert, H. F. (1993) Guanidine hydrochloride stabilization of a partially unfolded intermediate during the reversible denaturation of protein disulfide isomerase. *Proc. Natl. Acad. Sci. U. S. A.* 90, 2107–2111.
- (34) Morrow, J. A., Segall, M. L., Lund-Katz, S., Phillips, M. C., Knapp, M., Rupp, B., and Weisgraber, K. H. (2000) Differences in stability among the human apolipoprotein E isoforms determined by the amino-terminal domain. *Biochemistry* 39, 11657–11666.
- (35) Dergunov, A. D. (2011) Local/bulk determinants of conformational stability of exchangeable apolipoproteins. *Biochim. Biophys. Acta* 1016/j.bbapap.2011.05.001.
- (36) Clement-Collin, V., Barbier, A., Dergunov, A. D., Visvikis, A., Siest, G., Desmadril, M., Takahashi, M., and Aggerbeck, L. P. (2006) The structure of human apolipoprotein E2, E3 and E4 in solution. 2. Multidomain organization correlates with the stability of apoE structure. *Biophys. Chem.* 119, 170–185.
- (37) Segall, M. L., Dhanasekaran, P., Baldwin, F., Anantharamaiah, G. M., Weisgraber, K. H., Phillips, M. C., and Lund-Katz, S. (2002) Influence of apoE domain structure and polymorphism on the kinetics of phospholipid vesicle solubilization. *J. Lipid Res.* 43, 1688–1700.
- (38) Narayanaswami, V., Kiss, R. S., and Weers, P. M. (2010) The helix bundle: a reversible lipid binding motif. *Comp. Biochem. Physiol., Part A: Mol. Integr. Physiol.* 155, 123–133.
- (39) Tanaka, M., Dhanasekaran, P., Nguyen, D., Nickel, M., Takechi, Y., Lund-Katz, S., Phillips, M. C., and Saito, H. (2011) Influence of N-terminal helix bundle stability on the lipid-binding properties of human apolipoprotein A-I. *Biochim. Biophys. Acta* 1811, 25–30.
- (40) Pownall, H., Pao, Q., Hickson, D., Sparrow, J. T., Kusserow, S. K., and Massey, J. B. (1981) Kinetics and mechanism of association of human plasma apolipoproteins with dimyristoylphosphatidylcholine: effect of protein structure and lipid clusters on reaction rates. *Biochemistry* 20, 6630–6635.
- (41) Peters-Libeu, C. A., Newhouse, Y., Hall, S. C., Witkowska, H. E., and Weisgraber, K. H. (2007) Apolipoprotein E\*<sup>2</sup> dipalmitoylphosphatidylcholine particles are ellipsoidal in solution. *J. Lipid Res.* 48, 1035–1044.
- (42) Schneeweis, L. A., Koppaka, V., Lund-Katz, S., Phillips, M. C., and Axelsen, P. H. (2005) Structural Analysis of Lipoprotein E Particles. *Biochemistry* 44, 12525–12534.
- (43) Kim, J., Basak, J. M., and Holtzman, D. M. (2009) The Role of Apolipoprotein E in Alzheimer's Disease. *Neuron* 63, 287–303.
- (44) Sivashanmugam, A., and Wang, J. (2009) A unified scheme for initiation and conformational adaptation of human apolipoprotein E N-terminal domain upon lipoprotein binding and for receptor binding activity. *J. Biol. Chem.* 284, 14657–14666.
- (45) Lund-Katz, S., and Phillips, M. C. (2010) High density lipoprotein structure-function and role in reverse cholesterol transport. *Subcell. Biochem.* 51, 183–227.
- (46) Hatters, D. M., Zhong, N., Rutenber, E., and Weisgraber, K. H. (2006) Amino-terminal domain stability mediates apolipoprotein E aggregation into neurotoxic fibrils. *J. Mol. Biol.* 361, 932–944.
- (47) DeKroon, R. M., and Armati, P. J. (2001) The Endosomal Trafficking of Apolipoprotein E3 and E4 in Cultured Human Brain Neurons and Astrocytes. *Neurobiol. Dis.* 8, 78–89.
- (48) Ramaswamy, G., Xu, Q., Huang, Y., and Weisgraber, K. H. (2005) Effect of domain interaction on apolipoprotein E levels in mouse brain. *J. Neurosci.* 25, 10658–10663.
- (49) Riddell, D. R., Zhou, H., Atchison, K., Warwick, H. K., Atkinson, P. J., Jefferson, J., Xu, L., Aschmies, S., Kirksey, Y., Hu, Y., Wagner, E., Parratt, A., Xu, J., Li, Z., Zaleska, M. M., Jacobsen, J. S., Pangalos, M. N., and Reinhart, P. H. (2008) Impact of apolipoprotein E (ApoE) polymorphism on brain ApoE levels. *J. Neurosci.* 28, 11445–11453.
- (50) LaDu, M. J., Falduto, M. T., Manelli, A. M., Reardon, C. A., Getz, G. S., and Frail, D. E. (1994) Isoform-specific binding of apolipoprotein E to beta-amyloid. *J. Biol. Chem.* 269, 23403–23406.
- (51) Tamamizu-Kato, S., Cohen, J. K., Drake, C. B., Kosaraju, M. G., Drury, J., and Narayanaswami, V. (2008) Interaction with Amyloid beta Peptide Compromises the Lipid Binding Function of Apolipoprotein E. *Biochemistry* 47, 5225–5234.
- (52) Santoro, M. M., and Bolen, D. W. (1988) Unfolding free energy changes determined by the linear extrapolation method. 1. Unfolding of phenylmethanesulfonyl alpha-chymotrypsin using different denaturants. *Biochemistry* 27, 8063–8068.
- (53) Johnson, K. A., Simpson, Z. B., and Blom, T. (2009) FitSpace explorer: an algorithm to evaluate multidimensional parameter space in fitting kinetic data. *Anal. Biochem.* 387, 30–41.